ACS APPLIED MATERIALS & INTERFACES

Research Article

www.acsami.org

Optical Sensing of the Ionic Strength Using Photonic Crystals in a Hydrogel Matrix

Christoph Fenzl, Stefan Wilhelm, Thomas Hirsch,* and Otto S. Wolfbeis

Institute of Analytical Chemistry, Chemo- and Biosensors, University of Regensburg, 93040 Regensburg, Germany

Supporting Information

ABSTRACT: Monodisperse, highly negatively charged, cross-linked polystyrene nanoparticles with diameters between 80 and 120 nm have been incorporated into a polyacrylamide hydrogel, where they display an iridescent color that conventionally is attributed to the so-called photonic crystal effect. The film is of red color if placed in plain water but turns to green in the presence of a 1 mM solution of an electrolyte such as sodium chloride and to purple in 100 mM solutions of electrolytes. Quantitative reflection spectroscopy was performed at various wavelengths and resulted in plots of reflected light wavelength versus ionic strength (IS) that are almost linear in the logarithmic concentration range from 5×10^{-5} to 10^{-2} mol·L^{-1}. We show that such films are capable of monitoring the IS of aqueous solutions in the pH range from 5 to 9. We also show that, in addition to visual and instrumental readout, the sensor films can be analyzed with a digital camera at fixed angle. The digital images were separated into their red, green, and blue channels and analyzed. The red channel was found to be best suited for determination of the IS and resulted in calibration plots that are comparable if not better than those obtained by reflectometry.

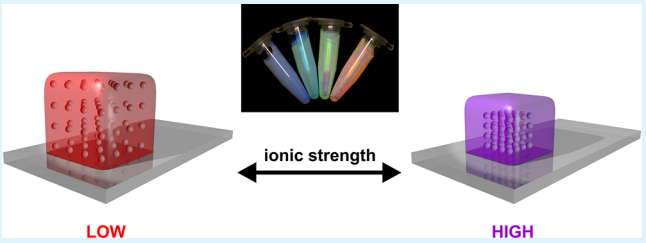

KEYWORDS: *photonic crystal, ionic strength, sensor, hydrogel, RGB readout, nanoparticles*

INTRODUCTION

The term "photonic crystals" (PhCs) relates to a periodical arrangement of a regularly shaped, often transparent material consisting of nanoparticles and polymer that differ in their dielectric constants. In perfect PhCs, light of only a certain wavelength can propagate through their lattice.[1−3] Three-dimensional PhCs are characterized by periodicity in all three dimensions. Both top-down approaches and chemical bottom-up methods are known to create PhCs.[4−8] The latter are more simple and less expensive. In the preferred method, nanoscopic, monodisperse spheres are self-assembled to form PhCs.[9,10] Typical spheres include those made of silica, zinc oxide, titanium dioxide, or organic polymers such as polystyrene or poly(methyl methacrylate).[11−15] Among the common methods to generate a three-dimensional arrangement, sedimentation and electrostatic repulsion are particularly attractive.[16,17]

PhCs have been converted to sensor elements because their reflected wavelength depends on variables than can be altered by external stimuli. For example, the maximum wavelength of reflected light changes if the angle of incidence (or the orientation of the crystal array) is altered. Hence, this wavelength can be used to verify the orientation of the PhC.[18,19] The particle spacing and their refractive index are two other variables that can cause a change in the reflected wavelength. Although both often vary simultaneously, the relative change in the distance is usually more expressed than that of the refractive index.[20] If the initial distance between the particles is fixed by placing them in a fairly rigid polymer, changes in the wavelength can be observed if the matrix swells or shrinks.[21]

There are two fundamental types of chemically responsive PhCs: The first is based on porous structures with tunable refractive indices and the second on shrinking and swelling of the polymers. The first type is a good choice if solvents of different refractive indices are to be discerned. Materials with inverse opal structure, such as oxides of silicon, aluminum, tin, and zirconium,[22,23] show a significant response, which, however, is not selective for the respective solvent.[24,25] Reduction of the pore size improves the sensitivity and selectivity so that, for example, the so-called mesoporous Bragg stacks consisting of TiO_2 and SiO_2 can differentiate between alcohols and alkanes despite their similar refractive indices.[26,27]

The second type of chemoresponsive PhCs forms the larger basis for sensor applications. A polyacrylamide hydrogel film containing polystyrene nanoparticles was shown[28] to optically respond to pH values and to undergo a fully reversible wavelength shift of around 250 nm on changing from pH 2 to 7. It was also noted that the ionic strength (IS) interferes, but this was not studied in detail even though this represents a rather adverse effect in a pH sensor. Ion-selective PhC-based sensors for potassium[21] and lead[29−31] have been reported that utilize certain crown ethers. Mercury ions were sensed[32] using the enzyme urease because it is inhibited by such ions.

Received: October 16, 2012
Accepted: December 4, 2012
Published: December 4, 2012

Wavelength shifts of up to 250 nm were observed. Glucose can be detected by a sensor with boronic acids.[33,34] Creatinine-sensing PhCs are making use of the enzyme creatinine deiminase,[35] but diffraction shifts remain small. The literature recently discussed possible future combinations of PhC biosensors with high-throughput screening and immunoassays.[36,37]

Sensors for the IS are needed in various fields of science and technology, for example, for monitoring of the salinity of marine and estuary waters, in fish agriculture, during blood dialysis, and in the chemical industry. Optical sensors for the IS are known[38] but require sophisticated indicator probes and instrumental readout. A sensor element that enables bare-eye inspection obviously would have numerous merits. However, such sensors have to be specific and must not be interfered with by pH values or dissolved oxygen or carbon dioxide. We report here on a sensor for the IS that has these merits. It is based on monodisperse nanoparticles possessing high surface charge that facilitate their periodic arrangement to give the desired photonic effect. The nanospheres are incorporated into an ion-permeable hydrophilic gel matrix in order to fix them in their position. The resulting sensor films are examined with respect to sensitivity, selectivity, and potential sensor applications. We also present a method for readout using a commercial digital camera.

EXPERIMENTAL METHODS

Synthesis of Poly(styrene-*co*-sodium styrenesulfonate) Nanoparticles. A mixture of styrene (18.8 g; Sigma-Aldrich, >99%) and divinylbenzene (DVB; 1.2 g; Sigma-Aldrich, technical grade, 80%) was added to a volume of 152 mL of ultrapure and oxygen-free water (0.055 $\mu S \cdot cm^{-1}$) using a syringe. The turbid emulsion was stirred at 300 rpm and heated to a temperature of 91 °C with an oil bath. Next, a solution of 203 mg of sodium styrenesulfonate (Sigma-Aldrich, technical grade) in 5 mL of water was added. After 3 min, 5 mL of an aqueous solution containing 29 mg of sodium bicarbonate and 76 mg of sodium persulfate ($Na_2S_2O_8$) was injected to initiate polymerization. After 25 min, 10 mL of water and a second batch of monomers were added in the following order: (1) a mixture of 3.76 g of styrene and 240 mg of DVB, (2) a solution of 1 g of styrenesulfonate in 5 mL of water, and (3) 5 mL of the aqueous initiator solution, which was injected. After 1 h, the reaction was complete, the oil bath removed, and the mixture allowed to cool to room temperature. The milky suspension was filtered through a double layer of filter paper. For purification, 50 mL of a crude nanoparticle suspension was equally distributed into 10 polycarbonate centrifugation vials, and all were centrifuged for 90 min at a relative centrifugal force (RCF) of 49000*g*. The resulting pellets were suspended in 5 mL of water by vortexing and ultrasonic treatment. This procedure was repeated, and the resulting emulsion was centrifuged again for 180 min (RCF 49000*g*) and redispersed in 5 mL of water. The centrifuged suspension of nanoparticles was diluted with 50 mL of water and the temperature of the mixture maintained at 85 °C. After 3 days, the emulsion was cooled to room temperature and again centrifuged according to the protocol described before. The resulting iridescent suspension was kept under nitrogen for storage.[39]

Preparation of a Polyacrylamide Hydrogel Based Polymerized Colloidal Crystal Array Film (PCCA Film). Acrylamide (50 mg; Sigma-Aldrich, >99%) and *N*,*N*′-methylenediacrylamide (3.5 mg; Merck, for electrophoresis) were dissolved in a suspension of 1 mL of poly(styrene-*co*-sodium styrenesulfonate) nanoparticles (60 $g \cdot L^{-1}$) in ultrapure water. A solution of 10 μL of 2,2-diethoxyacetophenone (Sigma-Aldrich, >95%) in 10 μL of dimethyl sulfoxide and 165 mg of AG-501 X8 ion-exchange resin (BIO-RAD, Hercules, CA, biotechnical grade) was added. After intense vortexing, nitrogen was bubbled through the mixture to remove oxygen. The suspension was injected into a polymerization cell consisting of two microscope slides and side walls consisting of a Parafilm spacer with a thickness of 125 μm. Photopolymerization was carried out by UV irradiation at 366 nm (6 W) for 5 h, after which the gel was fully polymerized but not yet dry. The film was washed several times with water and transferred to a glass slide. In order to hydrolyze the amino group to form carboxylate groups, a mixture of 900 μL of 1 M sodium hydroxide and 100 μL of *N*,*N*,*N*′,*N*′-tetramethylethylenediamine (Serva, Heidelberg, Germany, >99%) was poured over the film. After 4 min of hydrolysis, the film was thoroughly washed with ultrapure water.[28]

Particle Size [Transmission Electron Microscopy (TEM) and Dynamic Light Scattering (DLS)] and Surface Charge Studies. The purified particles were dispersed (~8 $g \cdot L^{-1}$) in water and vortexed to obtain homogeneous suspensions. A carbon-coated copper grid was coated with a 10 μL drop of the suspension. After drying, micrographs were acquired with a transmission electron microscope (type CM 12 from Philips, Hamburg, Germany). DLS measurements were performed on the same suspensions. A disposable polystyrene cuvette was filled with 1 mL of the suspension and analyzed with a particle sizer in the backscattering mode at an angle of 173° (Zetasizer nano series, Malvern, www.malvern.com) at 20 °C after an equilibration time of 60 s. The autocorrelation of the intensity recorded over time is related to the geometry of the particles under observation. After 20 consecutive measurements, the mean hydrodynamic radius and the polydispersity index (PDI) were extracted from the autocorrelation data.

The electrophoretic mobility of the polystyrene nanospheres was measured by dispersing them at a concentration of approximately 8 $g \cdot L^{-1}$ in a 10 mM sodium chloride solution after prolonged vortexing. A folded capillary cell (type DTS1060 from Malvern) was charged with around 800 μL of the particle suspension and equilibrated to 20 °C for 60 s. The mean electrophoretic mobility was determined by laser Doppler velocimetry in 400 runs with the Zetasizer nano series. The Smoluchowski model was employed to determine the ζ potential of the dispersions. The surface charge of the particle suspensions was calculated via the relationship between the ζ potential (measured by determining the electrophoretic mobility of the colloidal dispersions) and the surface charge density, as described by Ohsawa et al.[40] and Ohshima et al.[41]

Measurements of the Reflected Light of PCCAs. The partially hydrolyzed polyacrylamide films containing polystyrene nanoparticles were placed on a microscope glass slide. Then, 500 μL amounts of solutions of varying salt concentration were placed on the hydrogel. The effect of the temperature was studied by immersing the film into a water-filled Petri dish, whose temperature was adjusted to values between 4 and 60 °C. The effects of the pH were measured by the same technique and by adjusting the respective pH values. A xenon lamp (0.5 W) was used as an illumination source, and an optical fiber waveguide was fixed at an angle of 90° with respect to the lamp. The fiber was connected to a USB 4000 spectrometer (Ocean Optics, Dunedin, FL, www.oceanoptics.com). Reflection spectra were recorded with SpectraSuite (from Ocean Optics, Dunedin, FL, www.oceanoptics.com) in reflectance mode with an integration time of 100 ms per spectrum. All measurements, except for the temperature study, were performed under ambient conditions at room temperature.

Digital Camera Readout of Sensor Films. A printed sheet of paper with the reference colors for the red, blue, and green channels was placed next to the polymer film. A digital single lens reflex camera (Canon EOS 60D) with a macro lens (Canon EF 100 L IS USM) was fixed at an angle of 90° with respect to the light source (a 60 W standard light bulb), which was kept in a fixed position, thereby maintaining the white balance of the camera at a constant color temperature of 3200 K. The exposure time was 0.1 s, and the aperture was adjusted to f/6.3. All images were recorded in the JPEG format. The color channels were separated with the software *ImageJ* (freeware available at http://rsbweb.nih.gov/ij/index.html). The mean intensity of a square consisting of 90000 pixels of the polymer film was determined for each channel. In order to balance possible changes in the light conditions, a square of the same size was also analyzed for the respective reference color for the red, green, and blue channels.

RESULTS AND DISCUSSION

Choice of Materials. Three-dimensional PhCs can be constructed fairly easily via the controlled arrangement of periodic dielectric, highly monodisperse spheres. Critical factors in terms of materials include (a) the properties of the dielectric material and (b) the ability of the material to assemble with appropriate spacing so as to enable a spectrally pure diffraction of visible light. The introduction of charged groups on the surface of the nanoparticles is a good means to control their arrangement. Nanoparticles made from styrene have the advantage of a refractive index (1.59) that differs significantly from that of air or water, which is a desirable property for PhCs. Styrene can easily be polymerized and cross-linked, and its size and polydispersity can be governed with the aid of surfactants. Sulfo groups can be introduced by adding styrenesulfonate as a second monomer. The quantities employed (see the Experimental Methods section) are the result of an optimization based on variation of the concentrations of the cross-linker and initiator and polymerization time. Surface charge exerts a large influence: too low a surface charge leads to nonvisible reflection because reflected light is in the UV, while too high a surface charge leads to the opposite effect in that the wavelength of the reflected light becomes too long and films appear colorless.

Polyacrylamide, in turn, was chosen as a sensor matrix because it is permeable to ions and because all of the components are water-soluble and transparent, so the iridescent colors of the colloidal crystal dispersions are not impeded. Interestingly, it was found that polyacrylamide alone as a matrix material does not render the film sensitive to the IS unless the amido groups are (at least partially) hydrolyzed to form carboxy groups ($pK_a \sim 4$). This makes the materials sensitive to pH values of <5, as will be shown below, which is, however, outside the pH ranges where the IS is usually determined (pH 5–9).

Characterization of Polystyrene Nanoparticles. TEM pictures and the results of the DLS measurements were acquired and compared. As expected, the hydrodynamic radius obtained by DLS is larger than the physical radius obtained by TEM because a high surface charge will lead to an extended hydration shell, which causes the particle to appear larger in scattering experiments. The mean diameter, measured by the evaluation of 376 particles in the TEM image (Figure 1), is 83 ± 9 nm (see Figure S5 in the Supporting Information), while a hydrodynamic diameter of 106 nm (with a PDI of 0.10) is found in DLS measurements. A surface charge of 3.3×10^3 elemental charges per particle has been calculated from the electrophoretic mobility data.

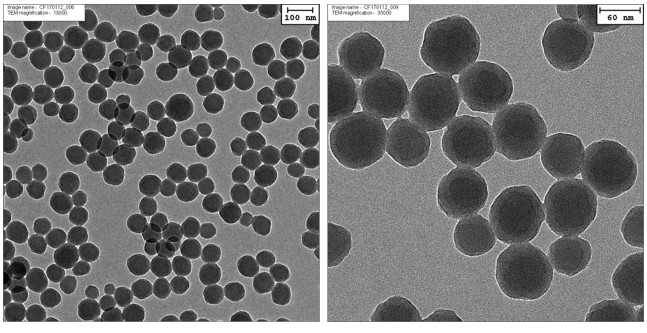

Figure 1. TEM images of monodisperse nanoparticles consisting of styrene, DVB, and sodium styrenesulfonate. The shell with the lighter color is obtained by the second polymerization step during synthesis.

One can assume that repulsive forces between particles increase with the number of charged groups per particle. For chemical sensor applications with colloidal PhCs embedded in a polymer matrix, it is desirable that the nanoparticle dispersions reflect visible light, so as to enable visual readout. In fact, the size and narrow distribution result in a strong violet reflectance of these films. The particles exhibit excellent long-term stability. After 6 months, an increase in the diameter of 4 nm and of the PDI of 0.04 was found, and this did not alter the optical properties of the particles in the hydrogel.

Sensor Properties of the PhC Films. On the basis of a remark made earlier,[28] we expected the PhC hydrogel films to be affected by the IS. In order to quantify this, films were immersed in solutions of varying salt concentrations at constant pH value, so the IS was adjusted with salts with several anions including sodium chloride, sodium sulfate, and sodium citrate. The concentrations of the solutions ranged from 10^{-6} to 10^{-1} mol·L^{-1}, corresponding to ISs in the range from 10^{-6} to 6×10^{-1} mol·L^{-1}. A plot of the maximum peak wavelength versus IS is given in Figure 2. The effect obviously is due to an IS-induced change in the distance between the charged nanoparticles. Unfortunately, a calculation of the lattice constants was found to be difficult because not only is the particle-to-particle distance changed upon increasing IS but also the refractive index of the incorporating (hydrogel) matrix.

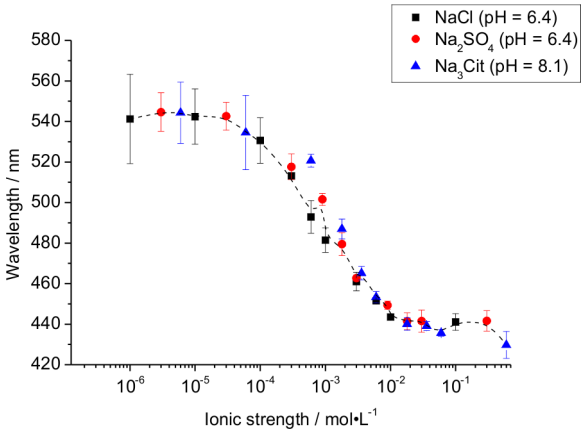

Figure 2. Effect of the IS on the wavelength of the reflected light of colloidal PhCs in a hydrolyzed polyacrylamide hydrogel immersed in salt solutions of sodium chloride (NaCl), sodium sulfate (Na_2SO_4), and sodium citrate (Na_3Cit) at varying concentrations. Each data point presents the average value of five measurements; the error bars indicate the standard deviation of these measurements. Also see Figure 3.

The peak wavelengths change with the IS between 5×10^{-5} and 2×10^{-2} mol·L^{-1}. The higher standard deviation in the low concentration range is due to errors caused by the high dilution of the stock solutions. Signal changes are fully reversible, and the response times are <1 s. This is much faster than the signal changes reported by Lee and Braun for tunable inverse opal hydrogel pH sensors, which show reversibility only within 1200 s.[42] In the linear range of the logarithmic scale (10^{-4}–10^{-2} mol·L^{-1}), a change of 1 order of magnitude in the IS leads to a 50 nm shift in the wavelength. Given the strong correlation in the color of the modified hydrogel in solutions to the IS, quantification by digital photography analysis was attempted. Details on the acquisition of the pictures and on data processing are given in the Supporting Information. Pictures

dx.doi.org/10.1021/am302355g | ACS Appl. Mater. Interfaces 2013, 5, 173–178

of sensor films in solutions of different ISs are shown in Figure 3. The variations in the coloration result from the fact that the

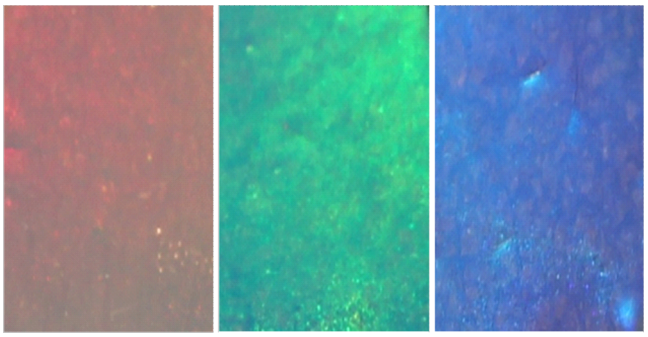

Figure 3. Colors of a sensor layer composed of a polyacrylamide hydrogel matrix containing colloidal PhCs. Left: Color in pure water (red), Center: color in a sodium chloride solution (10^{-3} mol·L^{-1}; green). Right: Color at c(NaCl) = 10^{-1} mol·L^{-1} (purple).

film is not completely smooth so that light is reflected in slightly different ways. The reflection spectra recorded with fiber optics were uniform over the whole area.

Analysis of the red channel of the camera yields a linear range in the logarithmic scale that lies between 10^{-4} and 10^{-3} mol·L^{-1} IS, which causes a shift in the relative intensity of 42% between these two concentrations (Figure 4). The error margins are

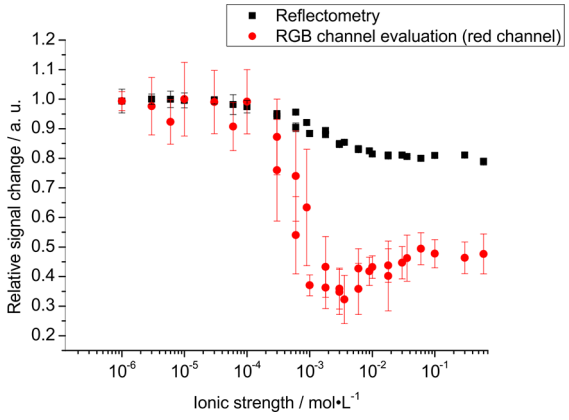

Figure 4. Relative signal changes as measured by reflectometry (black squares) and by analysis of the red channel of the corresponding picture (red circles) at varying ISs.

acceptable, and the form of the curve resembles that obtained by reflection measurements. Note: The (seemingly) large error bars do not reflect the resolution of this method but rather the batch variation from sensor to sensor, with these resulting from measurements with five different films prepared by the same protocol. The standard deviation obtained when using a single film for several measurements is, in fact, negligibly small. The color information of the red channel seems best suited to determine the IS via red−green−blue (RGB) readout of photographs.

In order to validate that the camera method is a reliable alternative, the reflectometric signals and those of the red channel of the photographs were normalized (Figure 4). The relative signal change obtained by RGB analysis is distinctly higher than that obtained by reflectometry. These results show the potential of colloidal PhCs in a hydrogel matrix to simply determine the IS (salinity) of an aqueous sample.

Interferences may be caused by changes in the pH and temperature. Therefore, the effect of the pH (using the monoprotic acid hydrochloric acid and the diprotic acid sulfuric acid for acidification) on the reflectivity of the PCCA film was studied, and the results were compared to those caused by sodium chloride (Figure 5). One can clearly see that both acids also exert an effect at pH values below 5, which is, however, outside the range of pH values encountered in biology and marine sciences. The response to the pH reported here does not coincide with that reported in ref28, but this does not come as a surprise because the response of such sensors to pH values strongly depends the composition of the particles and the (partially hydrolyzed) hydrogel.

We assume that the effect caused by the acids is due to (a) protonation of the carboxy groups of the (partially hydrolyzed) hydrogel and (b) an increase of the IS (both acids are fully dissociated at such pH values). The slope of the plot for hydrochloric acid is steeper than that for NaCl. A comparison of hydrochloric acid and sulfuric acid reveals that they cause an effect only at pH values between 3.5 and 4.5. This correlates well with the pK_a of the carboxy groups of the partially hydrolyzed polyacrylamide. As a result, this sensor is adequate for sensing the IS at pH values >5 and thus well suited for biological systems, where the IS exerts a strong effect, for example, on the reaction rates of enzymes.

The sensor layers also were examined for the effect of the temperature in the range from 4 to 60 °C (see Figure S4 in the Supporting Information). The signal was found to remain

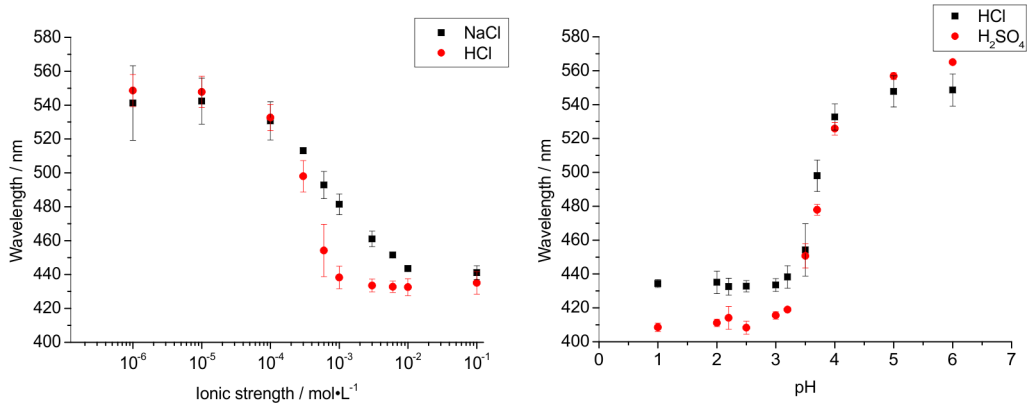

Figure 5. Comparison of the reflected wavelength of a hydrolyzed PCCA film immersed in solutions of NaCl, HCl, and H_2SO_4 at various ISs (left) and pH values (right).

dx.doi.org/10.1021/am302355g | ACS Appl. Mater. Interfaces 2013, 5, 173−178

constant over the full course of heating and cooling, implying that swelling or shrinking due to the temperature can be neglected over the entire temperature range. We also find no differences in the response to IS if the sensor is examined in solutions saturated with air or nitrogen.

Precision. Shifts in the peak wavelength of the reflected light can typically be determined with a precision of ±1 nm. This is equivalent to a sensitivity (slope) of about 0.03 logarithmic units in the linear part of the logarithmic calibration plot (from 10^{-4} to 10^{-2} mol·L^{-1}). In other words, one can clearly distinguish between the ISs of 100 and 104 μM. Shifts in the maximum of the reflectance spectrum (see Figure S2 in the Supporting Information) can be determined with even higher precision by fitting, but this was not attempted here because the resolution of the sensor already is adequate. In the case of RGB readout, the results are similar. Here, the color information of 90000 pixels was used to obtain the signal. This information was taken in relation to a reference image of the same number of pixels. Each channel has 255 distinct intensity steps. The change of one unit is equivalent to 0.56% of the relative intensity scale, as displayed in Figure S1 in the Supporting Information. Therefore, the precision in the determination of the IS is 0.036 logarithmic units. In other words, the sensitivity is about 3 times better in this method compared to the reflectometry.

CONCLUSION

The hydrogel-based PhC sensor presented here is capable of sensing IS over a wide range by giving very distinct color changes. It is not affected by the temperature and by pH values higher than 5.0 (see Figure S3 in the Supporting Information). An increase in the IS on going from 10^{-4} to 10^{-3} mol·L^{-1} solutions results in a wavelength shift of 50 nm and a change in color from red to purple. The sensor enables bare-eye readout but also RGB analysis via a digital camera. This facilitates quantization based on the 42% decrease in the relative intensity of the red channel. Other features include a fast response time, full reversibility, and a complete lack of photobleaching.

ASSOCIATED CONTENT

Supporting Information

Experimental details on the acquisition of the pictures and on data processing, UV−vis reflection spectra of PCCA films, the pH and temperature dependencies of the reflected wavelength of PCCA films, and particle-size determination with TEM. This material is available free of charge via the Internet at http://pubs.acs.org.

AUTHOR INFORMATION

Corresponding Author

*E-mail: thomas.hirsch@ur.de.

Notes

The authors declare no competing financial interest.

ACKNOWLEDGMENTS

This study was partially financed by the Sensor Applikations-zentrum Regensburg (see www.sappz.de).

REFERENCES

(1) Joannopoulos, J. D.; Johnson, S. G.; Winn, J. N.; Meade, R. D. *Photonic Crystals: Molding the Flow of Light*, 2nd ed.; Princeton University Press: Princeton, NJ, 2008; p 2.
(2) Yablonovitch, E. *Phys. Rev. Lett.* **1987**, *58*, 2059−2062.
(3) John, S. *Phys. Rev. Lett.* **1987**, *58*, 2486−2489.
(4) Lin, S. Y.; Fleming, J. G.; Hetherington, D. L.; Smith, B. K.; Biswas, R.; Ho, K. M.; Sigalas, M. M.; Zubrzycki, W.; Kurtz, S. R.; Bur, J. *Nature* **1998**, *394*, 251−253.
(5) Fleming, J. G.; Lin, S.-Y. *Opt. Lett.* **1999**, *24*, 49−51.
(6) Noda, S.; Tomoda, K.; Yamamoto, N.; Chutinan, A. *Science* **2000**, *289*, 604−606.
(7) Ogawa, S.; Imada, M.; Yoshimoto, S.; Okano, M.; Noda, S. *Science* **2004**, *305*, 227−229.
(8) Wang, Z.; Zhang, J.; Xie, J.; Yin, Y.; Wang, Z.; Shen, H.; Li, Y.; Li, J.; Liang, S.; Cui, L.; Zhang, L.; Zhang, H.; Yang, B. *ACS Appl. Mater. Interfaces* **2012**, *4*, 1397−1403.
(9) Marlow, F.; Muldarisnur Sharifi, P.; Brinkmann, R.; Mendive, C. *Angew. Chem., Int. Ed.* **2009**, *48*, 6212−6233.
(10) Xia, Y.; Gates, B.; Yin, Y.; Lu, Y. *Adv. Mater.* **2000**, *12*, 693−713.
(11) Ge, J.; Yin, Y. *Angew. Chem., Int. Ed.* **2011**, *50*, 1492−1522.
(12) Aguirre, C. I.; Reguera, E.; Stein, A. *ACS Appl. Mater. Interfaces* **2010**, *2*, 3257−3262.
(13) Iler, R. K. *The Chemistry of Silica—Solubility, Polymerization, Colloid and Surface Properties, and Biochemistry*; John Wiley & Sons: New York, 1979; pp 172−461.
(14) Stöber, W.; Fink, A.; Bohn, E. *J. Colloid Interface Sci.* **1968**, *26*, 62−69.
(15) Matijevic, E. *Langmuir* **1994**, *10*, 8−16.
(16) Pieranski, P. *Contemp. Phys.* **1983**, *24*, 25−73.
(17) Van Negen, W.; Shook, I. *Adv. Colloid Interface Sci.* **1984**, *21*, 119−194.
(18) Kim, S.-H.; Jeon, S.-J.; Jeong, W. C.; Park, H. S.; Yang, S.-M. *Adv. Mater.* **2008**, *20*, 4129−4134.
(19) Ge, J.; Lee, H.; He, L.; Kim, J.; Lu, Z.; Kim, H.; Goebl, J.; Kwon, S.; Yin, Y. *J. Am. Chem. Soc.* **2009**, *131*, 15687−15694.
(20) Zhao, Y.; Xie, Z.; Gu, H.; Zhu, C.; Gu, Z. *Chem. Soc. Rev.* **2012**, *41*, 3297−3317.
(21) Saito, H.; Takeoka, Y.; Watanabe, M. *Chem. Commun.* **2003**, 2126−2127.
(22) Cai, Z.; Liu, Y.; Teng, J.; Lu, X. *ACS Appl. Mater. Interfaces* **2012**, *4*, 5562−5569.
(23) Yang, Z.; Gao, S.; Li, W.; Vlasko-Vlasov, V.; Welp, U.; Kwok, W.-K.; Xu, T. *ACS Appl. Mater. Interfaces* **2011**, *3*, 1101−1108.
(24) Bogomolov, V. N.; Gaponenko, S. V.; Germanenko, I. N.; Kapitonov, A. M.; Petrov, E. P.; Gaponenko, N. V.; Prokofiev, A. V.; Ponyavina, A. N.; Silvanovich, N. I.; Samoilovich, S. M. *Phys. Rev. E* **1997**, *55*, 7619−7625.
(25) Blanford, C. F.; Schroden, R. C.; Al-Daous, M.; Stein, A. *Adv. Mater.* **2001**, *13*, 26−29.
(26) Choi, S. Y.; Mamak, M.; von Freymann, G.; Chopra, N.; Ozin, G. A. *Nano Lett.* **2006**, *6*, 2456−2461.
(27) Fuertes, M. C.; López-Alcaraz, F. J.; Marchi, M. C.; Troiani, H. E.; Luca, V.; Míguez, H.; Soler-Illia, G. J. a. A. *Adv. Funct. Mater.* **2007**, *17*, 1247−1254.
(28) Lee, K.; Asher, S. A. *J. Am. Chem. Soc.* **2000**, *122*, 9534−9537.
(29) Holtz, J. H.; Asher, S. A. *Nature* **1997**, *389*, 829−832.
(30) Holtz, J. H.; Holtz, J. S. W.; Munro, C. H.; Asher, S. A. *Anal. Chem.* **1998**, *70*, 780−791.
(31) Reese, C. E.; Asher, S. A. *Anal. Chem.* **2003**, *75*, 3915−3918.
(32) Arunbabu, D.; Sannigrahi, A.; Jana, T. *Soft Matter* **2011**, *7*, 2592−2599.
(33) Asher, S. A.; Alexeev, V. L.; Goponenko, A. V.; Sharma, A. C.; Lednev, I. K.; Wilcox, C. S.; Finegold, D. N. *J. Am. Chem. Soc.* **2003**, *125*, 3322−3329.
(34) Alexeev, V. L.; Das, S.; Finegold, D. N.; Asher, S. A. *Clin. Chem.* **2004**, *50*, 2353−2360.
(35) Sharma, A. C.; Jana, T.; Kesavamoorthy, R.; Shi, L.; Virji, M. A.; Finegold, D. N.; Asher, S. A. *J. Am. Chem. Soc.* **2004**, *126*, 2971−2977.
(36) Heeres, J. T.; Hergenrother, P. J. *Chem. Soc. Rev.* **2011**, *40*, 4398−4410.
(37) Zhao, Y.; Zhao, X.; Gu, Z. *Adv. Funct. Mater.* **2010**, *20*, 2970−2988.

(38) Huber, C.; Klimant, I.; Krause, C.; Werner, T.; Mayr, T.; Wolfbeis, O. S. *Fresenius' J. Anal. Chem.* **2000**, *368*, 196−202.
(39) Sunkara, H. B.; Jethmalani, J. M.; Ford, W. T. *J. Polym. Sci., Part A: Polym. Chem.* **1994**, *32*, 1431−1435.
(40) Ohsawa, K.; Murata, M.; Ohshima, H. *Colloid Polym. Sci.* **1986**, *264*, 1005−1009.
(41) Ohshima, H.; Healy, T. W.; White, L. R. *J. Colloid Interface Sci.* **1982**, *90*, 17−26.
(42) Lee, Y.-J.; Braun, P. V. *Adv. Mater.* **2003**, *15*, 563−566.